

Exploring Effects of Homogenization on an OpenMC Depletion Analysis of a TRISO Fueled, Helium Cooled Microreactor

Lewis I. Gross^{1,*}, Patrick Shriwise^{2,1}, Benjamin Lindley¹, Paul P. H. Wilson¹

¹University of Wisconsin - Madison, Madison, Wisconsin; ²Argonne National Laboratory

[leave space for DOI, which will be inserted by ANS]

ABSTRACT

OpenMC is a state-of-the art, open-source Monte Carlo transport code. This work used OpenMC for depletion analysis of an infinite, unit cell model of the Virtual Test Bed gas-cooled microreactor. This microreactor is prismatic, TRISO-fueled, and helium gas cooled. Since the gas-cooled microreactor is intended for load-following, depletion analyses were conducted for 100%, 50%, and 10% of the rated power (225 kW_{th}) both for explicitly represented TRISO and volume-homogenized fuel compacts. This study aims to quantify the effects of homogenization on the k -eigenvalue and isotopics at shutdown. Modeling the unit cell will inform about the effects of homogenization on the system before moving on to a full-core model. The system eigenvalue, k_{inf} , was computed at each burnup step. The time steps selected ensure the same total burnup accrues at each step for each power level. A comparison of xenon-135 number density between each power is included for the homogenized cases, which is a key factor explaining the observed k_{inf} trends. With results for all fully explicit cases, a comparison of k_{inf} versus burnup between explicit and homogenized cases, as well as a comparison of the isotopics at shutdown will be included.

Keywords: OpenMC, TRISO, depletion, microreactor, gas-cooled

1. INTRODUCTION

For advanced reactors, especially those early in the design stage, sufficient modeling and simulation (M&S) are required to ensure the success of the design concept. Before any system can be built, modelers must prove systems perform safely. The Virtual Test Bed (VTB) [1] is a repository of reactor models used for research and demonstration of current tools in the nuclear industry as a part of the Nuclear Energy Advanced Modeling and Simulation (NEAMS) initiative. Various types of reactors are available on the VTB. Microreactors are one viable class of next generation systems with ongoing modeling efforts using NEAMS tools [2, 3]. One key advantage of microreactors is the ability to supply power to lower demand areas that may not be able to consume power on the order of a GW reactor or to areas needing temporary power, e.g. natural disaster relief efforts. While microreactors can be diverse in fuel, coolant, and general design, there is interest in combining high-temperature gas reactor (HTGR) and microreactor technologies. HTGRs have the benefits of higher electricity conversion efficiency from higher temperature coolant which synergizes with the desirable melting properties of tri-structural isotropic (TRISO) fuel. Adding these benefits to a microreactor bring many attractive features together.

Previous work on the VTB gas-cooled microreactor (GCMR) includes analysis of the system for a two day load-following transient [4]. This work coupled Griffin, BISON, and SAM using the Multiphysics

*ligross@wisc.edu

Object-Oriented Simulation Environment (MOOSE) framework. Griffin computed a solution to the neutron transport equation using a deterministic method, specifically the discrete ordinates and discontinuous finite element methods with the coarse mesh finite element method for acceleration. BISON is a fuel performance code that computed heat conduction in the solid parts of the system. SAM is a systems analysis code that computed heat transfer in the coolant channels.

Due to the smaller size of microreactors, it is conceivable to move the reactor at some point during operation, e.g. if the system was only needed temporarily or if power is needed elsewhere, or after shutdown but before refueling. In this case, for shielding and criticality safety reasons, the state of the core must be fully understood. If a system has been running on the order of months, the core composition has certainly changed since the initial loading due to the effects of depletion. Since Abdelhameed et al. only modeled 48 hours, depletion was not considered. Any analysis occurring far enough into an operation cycle requires a burnup simulation to know the state of isotopes in the core, whether computing an accident source term or shielding requirements for transporting the reactor after a shutdown. A few depletion studies of other microreactor concepts exist, though this work adds the first depletion analysis to the VTB GCMR. A study of the gas-cooled, Japanese High Temperature Test Reactor (HTTR) computed criticality and burnup using various cross section representations with SCALE6 and MCNP5/X [5]. Another study looked at burnup for Westinghouse's eVinci Heat Pipe Microreactor (HPMR), finding that it could operate for at least 10 years without refueling, despite making more sense as a nuclear battery over a centralized power source [6].

While previous work for the VTB GCMR used Griffin for neutron transport, this work chose OpenMC as an alternative to Griffin for a few reasons. First, OpenMC is an open-source (OS) code. For this study, as well as others wishing to verify any OpenMC simulation, the code is freely available to use. As a Monte Carlo code, there are advantages over a deterministic code, like Griffin, for depletion analysis. The microscopic cross sections in continuous energy format are more accurate when modeling the resonance region, as opposed to representing them with multi-group cross sections. There's also no need to do smaller studies to compute fine or coarse-group cross sections to produce diffusion coefficients with transport corrections for leakage – which is stronger in microreactors. OpenMC computes flux directly from continuous energy cross sections as an input to depletion.

The rest of this paper will be organized as follows. Section 2 will provide some background theory on depletion. Section 3 will detail the VTB GCMR and its components, explaining the OpenMC model and the depletion schemes. Section 4 will present results for the system. Section 5 will interpret those results and discuss the plans forward for more M&S.

2. DEPLETION THEORY

Once any reactor starts running, the composition of isotopes will change over time. Nuclides exposed to neutron flux will transmute into radioisotopes that have various modes of decay, creating new isotopes that did not exist at the start of operation, as well as decaying into other isotopes already in the system. The rate at which isotopes transmute and decay into each other depends on the transport solution via the reaction rates, which depend directly on the neutron flux. This relationship causes the coupling between transport and depletion to behave non-linearly [7].

Certain isotopes have more influence on the system than others. For example, xenon-135 has an extremely high neutron absorption cross section. It is so high that its negative reactivity insertion influences the positioning of the control elements. xenon-135 is particularly important in load-following contexts, in which the power changes once or twice per day, as its concentration increases when power decreases, and it is burned off when power increases again. This matters more in load-following contexts because the xenon-135 half-life is on the order of 9 hours [8]. For context, the load following schedule in Abdelhameed et al. has high power for 12 hours, low power for 7 hours, and 2.5 hour ramps between, inspired from the

NEA OECD report on load-following [4, 9].

To model burnup, transmutation and decay cross sections of the isotopes are combined with the computed flux to determine production and destruction rates for each isotope. These formulate a system of differential equations for the nuclide densities. For isotope i with number density $N_i(t)$, the Bateman or burnup equations describe the time dependent isotopic composition, given by

$$\frac{dN_i}{dt} = \sum_j \left[\int_0^\infty \sigma_{j \rightarrow i}(E, t) \phi(E, t) dE + \lambda_{j \rightarrow i} \right] N_j(t) - \left[\int_0^\infty \sigma_i(E, t) \phi(E, t) dE + \sum_j \lambda_{i \rightarrow j} \right] N_i(t), \quad (1)$$

where $\sigma_{j \rightarrow i}(E)$ is the transmutation cross section of isotope j that produces isotope i at energy E , and $\lambda_{j \rightarrow i}$ are the decay constants for decay modes in nuclide j that produce nuclide i . The system of equations for isotopes $i \in [1, n]$ can be expressed in matrix notation using the nuclide vector $\mathbf{n} \in \mathbb{R}^n$

$$\frac{d\mathbf{n}}{dt} = \mathbf{A}(\mathbf{n}, t)\mathbf{n} \quad \text{WITH} \quad \mathbf{n}(0) = \mathbf{n}_0, \quad (2)$$

where $\mathbf{A} \in \mathbb{R}^{n \times n}$ is the burnup matrix. Since the transport equation depends on number density and \mathbf{A} depends on the solution to the transport equation, \mathbf{A} then also depends on number density. Because “the timescale over which material compositions change is sufficiently long ... the transport equation can be solved as a steady-state equation” [7]. Taking the burnup equations as quasi steady-state allows the earlier non-separable equation to be solved via separation solution

$$\frac{d\mathbf{n}}{dt} = \mathbf{A}(\mathbf{n})\mathbf{n} \quad \text{WITH} \quad \mathbf{n}(0) = \mathbf{n}_0, \quad (3)$$

The solution to which is

$$\mathbf{n}(t) = e^{\mathbf{A}t} \mathbf{n}_0 \quad (4)$$

Solving Equation (3) and Equation (4) involves two separate components [7]:

1. Using a numerical method to integrate the matrix \mathbf{A} in Equation (3) forward in time. This usually involves taking one or more matrix exponential.
2. Evaluating the matrix exponential $\exp(\mathbf{A}t)$ or the action of the matrix exponential on a vector of nuclide concentrations.

There are various methods for time integration. Predictor-Corrector methods are commonly used for time integration in burnup contexts. In this study, the second order Constant-Extrapolation/Constant-Midpoint (CE/CM) is chosen, which is implemented by OpenMC and based on work comparing various integration schemes for depletion [10]. Since the method is second order, it requires two transport solves per depletion time step: one for the prediction and one for the correction. Using appropriate time steps for the quasi static assumption of burnup is also important. Namely, using smaller time steps when nuclide concentrations are expected to be changing more rapidly and larger time steps when nuclide concentrations are expected to be changing more slowly.

3. OPENMC MODEL

This section will describe the GCMR system and the corresponding OpenMC model. There are two parts to the model. The first assembles the geometry and material definitions. The second takes this model as input and defines a depletion simulation, facilitating the alternating transport, depletion, and nuclide updates.

3.1. System Description

Figure 1 shows a diagram of the GCMR. Graphite is the overall structural material of the unit cell with cylindrical compacts arranged in a hexagonal lattice. Table I shows various system parameters. The moderator uses YH_2 with a thin Cr coating encased in a FeCrAl envelope; the coating is between the YH_2 and the envelope. The poison compacts contain burnable B_4C spheres packed into graphite. The coolant uses helium. There is a top and bottom reflector made of BeO. Since the goal of this simulation is to determine excess reactivity, the B_4C control rod rests in the central compact of the upper reflector and is not inserted into the active core region, which instead is filled with non-circulating helium [4].

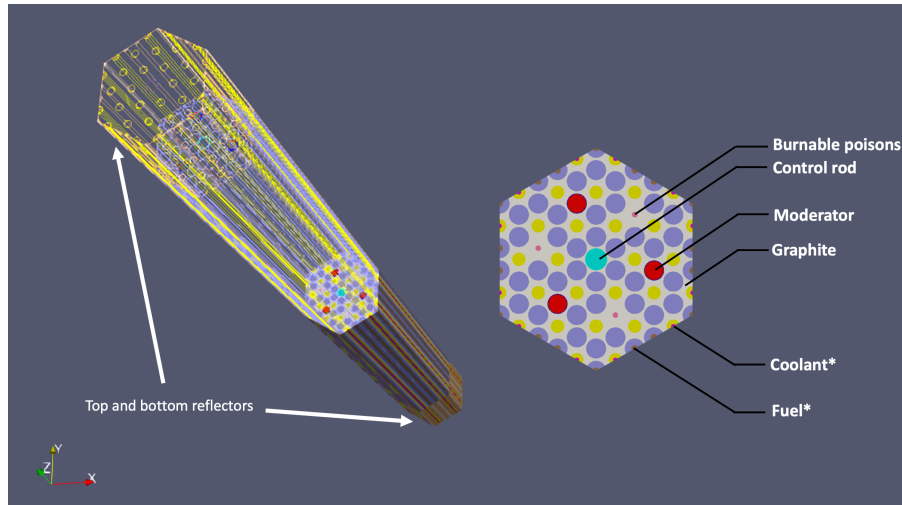


Figure 1. The above visualization shows the VTB GCMR unit cell: both a cross section of the fuel region and a 3D rendering of the fuel and reflectors [3].

fuel radius 0.90 cm	poison radius 0.25 cm	moderator radius, Cr coating 0.843 cm, 0.007 cm	control radius 0.99 cm	coolant radius 0.60 cm
FeCrAl thickness 0.05 cm	pin pitch 2.00 cm	fuel packing fraction 0.4 -	poison packing fraction 0.25 -	enrichment 19.95%

Table I. This table summarizes key dimensions of the compacts and parameters of the fuel and poison.

3.2. Model Definition

The system is divided into axial layers to compute spatial variation in flux. Since flux is a key input in to depletion, this allows depletion to also take advantage of the axial discretization and deplete at different rates accordingly. The axial division matched exactly the choice of [4], which includes two regions per reflector and 16 regions in the active fuel region. The heights of each region are 20 cm for each reflector and 160 cm for the fuel, which corresponds to each axial layer modeling 10 cm of the reactor. Figure 2 shows a radial slice of the fuel portion of the reactor. Figure 3 shows a radial slice of each reflector region.

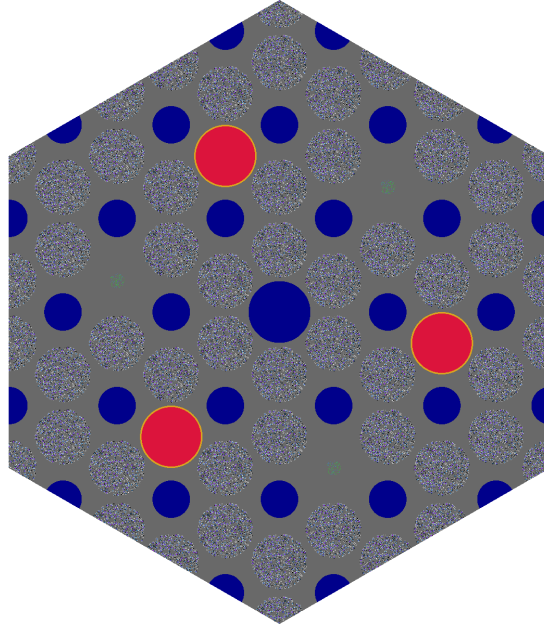
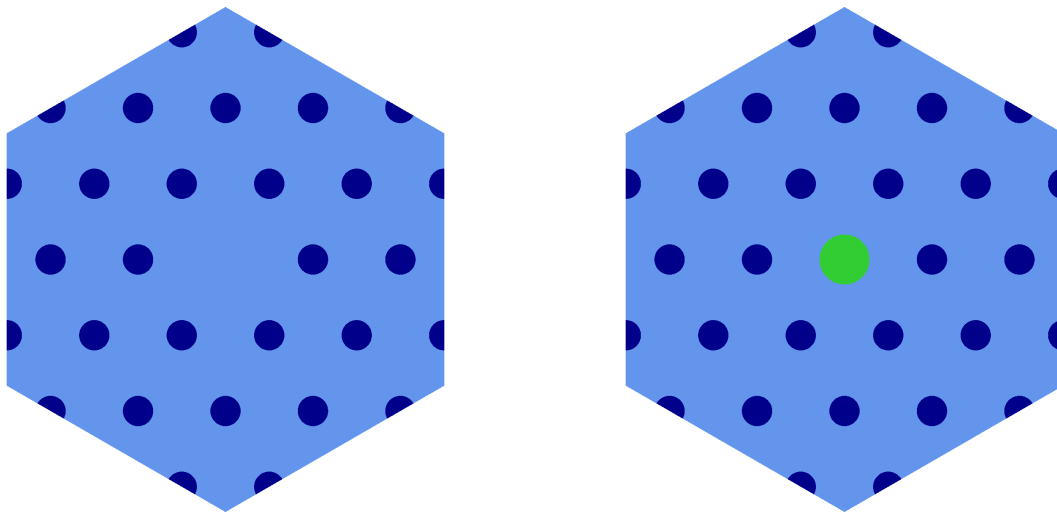


Figure 2. This figure shows a radial slice of the active region. Gray corresponds to graphite in the matrix or pyrolytic carbon, dark blue corresponds to helium coolant, red corresponds to YH_2 moderator, gold corresponds to FeCrAl, green corresponds to the B_4C poison particles (packed at 25 percent in graphite), and purple corresponds to the fuel kernel in the TRISO particles (packed at 40 percent in graphite).



(a) A slice of the lower reflector, colored by material. (b) A slice of the upper reflector, colored by material.

Figure 3. This figure shows a radial slice of the lower reflector (left) and the upper reflector (right). The difference between the upper and lower reflectors is that the upper reflector has an extra compact for the B_4C control rod. Dark blue corresponds to helium coolant and light blue corresponds to BeO, while the B_4C control rod is shown in green.

3.3. Depletion Simulation Definition

With complete geometry and material definitions, the depletion simulation defines power history, time steps, and an integration scheme. OpenMC then alternates between transport and Bateman equation solves. The cross sections used for transport are continuous energy from ENDF-B-VII.1. The chain file, an XML file used for depletion in OpenMC, contains transmutation and decay data necessary to compute the burnup matrix. This simulation used a chain based on the Consortium for Advanced Simulation of LWRs (CASL) project [11] and is provided by OpenMC [12]. While the chain originates from a light water reactor (LWR) system, the similarity of the neutron spectrum, i.e. both thermal, makes this chain file a good choice, since $\phi(E)$ is one of the inputs when computing the burnup matrix. The CASL chain can be found on OpenMC's website, specifically the portion that provides data for users to download.

In this work, the system is held at constant power for each case. This has some implications for the time stepping scheme chosen. To correctly account for the rapid build up of strong neutron absorbers, a few short initial time steps are included to increase those nuclides' accuracy. The time steps can be lengthened after this initial transient behavior, after allowing these important isotopes to reach a steady-state. Two different time steps were used for the results in Section 4. For the comparison at full power between explicit and homogenized cases, the time steps were as follows: three one-day time steps, three five-day time steps, and 23 fifteen-day time steps. For the comparison between all homogenized cases, three sets of time steps were used to ensure the same total burnup occurred at each step. The full power case used five one-day time steps, 3 five-day time steps, three fifteen-day time steps, and ten 60 day timesteps. The half and tenth power cases in this comparison use the same number of steps, with twice as long and ten times as long intervals, respectively.

4. RESULTS

There are a few metrics to compare between the different powers and TRISO representations. First, comparing the eigenvalue as a function of burnup gives a way to compare the effect of homogenization. Figure 4 shows results for the full power case of k_{inf} versus burnup for the time steps mentioned above. The full paper will show comparison for each power.

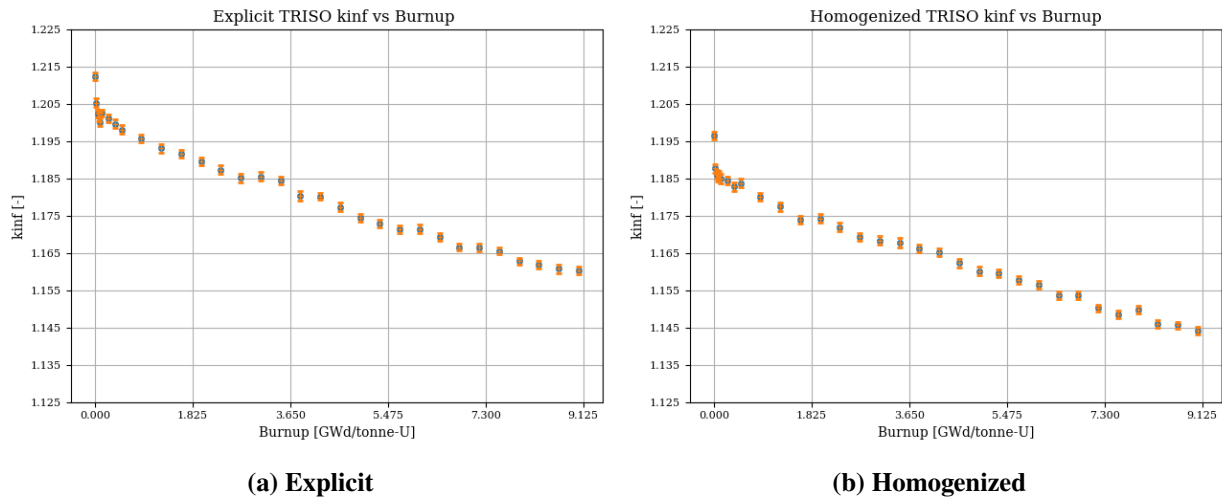


Figure 4. This figure compares k_{inf} for the explicit and homogenized fuel up to 9.125 GWd/tonne-U.

The above results are in line with theory on the effects of TRISO homogenization. The explicit case has a

noticeably higher eigenvalue caused by neutron interactions with the fuel. When the TRISO is explicitly represented, neutrons slow down significantly more before hitting fuel atoms and thus are more likely to cause fissions. In the homogenized case, the neutrons encounter uranium at higher energies and thus are more likely to be absorbed in the resonance region.

Next, Figure 5 shows k_{inf} for the homogenized cases, which shows the simulation's prediction of how the system will burnup at various powers. In order to explain the trends, it will be useful to examine the xenon-135 atom densities for each case, shown in Figure 6.

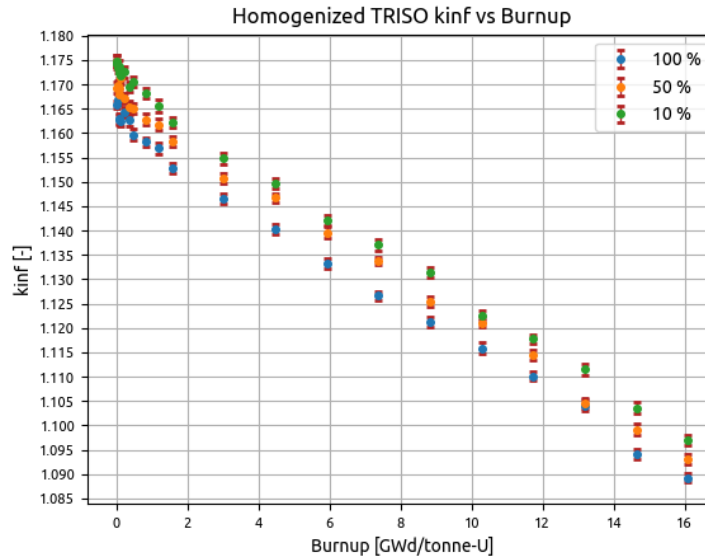


Figure 5. This figure compares k_{inf} for each power level among the volume homogenized fuel cases.

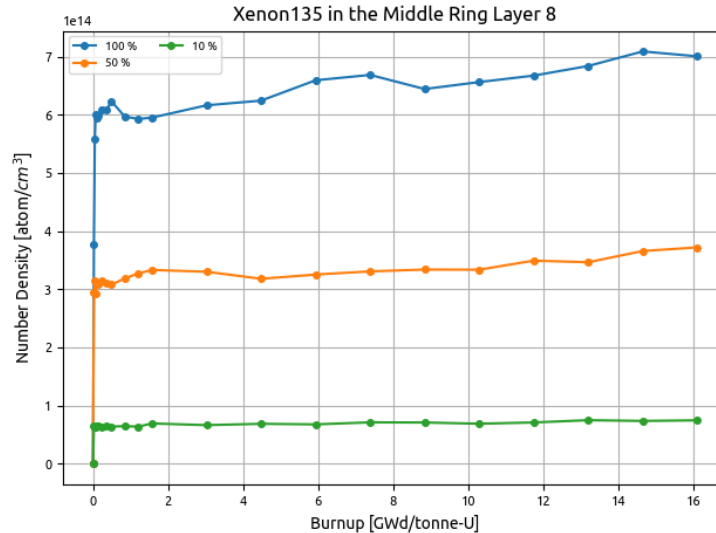


Figure 6. This figure shows xenon-135 atom density for each burnup step in the depletion simulation. The atom density shown here is for the 8th layer of 16 in the fuel region for one of the compacts in the innermost ring, around the control rod hole.

The above shows that the lower the power, the more excess reactivity is left at the end of the cycle, despite each time step using the same total burnup. All three systems start at $k_{inf} = 1.1748 \pm 0.0013$ but end up at $k_{inf} = 1.0893 \pm 0.0011$, $k_{inf} = 1.0931 \pm 0.0012$, and $k_{inf} = 1.0971 \pm 0.0012$ for full, half, and one-tenth power respectively. The xenon concentrations have an initial jump at start up and level out to equilibrium concentrations. The highest equilibrium concentration of xenon is at full power, and the equilibrium states lowers as power lowers. Since xenon-135 is a strong neutron poison, fuel has to compete with absorption in xenon. The stronger the xenon presence, the lower the eigenvalue will be with the same burnup (i.e. same total number of fuel atoms fissioned), explaining the observed trends between the homogenized cases.

5. CONCLUSIONS

This paper simulated the VTB GCMR, adding the first depletion analysis for the GCMR infinite, unit cell model. Since the reactor is intended to load follow, it depleted the system at 100%, 50% and 10% power. The k_{inf} versus burnup showed that the reactor still has excess reactivity for the explicit case after one year and after two years for all three homogenized cases. With explicit TRISO results for all powers, a comparison will inform on the effects of homogenization at each power level, including k_{inf} and the isotopics at shutdown. An important next step will be to model depletion during load following transients.

The software selected for future analyses will rely on Cardinal [13]. The Cardinal simulation will couple OpenMC for neutron transport, MOOSE's Heat Conduction Module (HCM) for heat conduction, and Thermal Hydraulics Module (THM) for 1-D thermal hydraulics. After standalone multiphysics work verification, the future goal is to couple depletion into the multiphysics algorithm to quantify the impact of depletion on high-fidelity multiphysics.

NOTE TO ORGANIZERS

Between now and the final deadline in January, there will be sufficient time to expand this analysis to hit the other power cases for the fully explicit case. Some results that are intended to be included are

- Longer depletion simulations (to find out when reactor goes subcritical)
- Isotopic comparison of important nuclides (^{235}U , ^{238}U , and ^{135}Xe) at the point when the reactor goes subcritical

ACKNOWLEDGEMENTS

The authors would like to thank the OpenMC development team for their guidance and assistance with software, as well as the Center for High Throughput Computing at the University of Wisconsin - Madison for their support in using the High Performance Cluster. The first author was supported in part by the US Nuclear Regulatory Commission's Graduate Fellowship Program administered by the University of Wisconsin-Madison.

REFERENCES

- [1] G. L. Giudicelli, A. Abou-Jaoude, A. J. Novak, A. Abdelhameed, P. Balestra, L. Charlot, J. Fang, B. Feng, T. Folk, R. Freile, T. Freyman, D. Gaston, L. Harbour, T. Hua, W. Jiang, N. Martin, Y. Miao, J. Miller, I. Naupa, D. O'Grady, D. Reger, E. Shemon, N. Stauff, M. Tano, S. Terlizzi, S. Walker, and C. Permann. "The Virtual Test Bed (VTB) Repository: A Library of Reference Reactor Models Using NEAMS Tools." *Nuclear Science and Engineering*, volume 0(0), pp. 1–17 (2023). URL <https://doi.org/10.1080/00295639.2022.2142440>.

- [2] N. E. Stauff, K. Mo, Y. Cao, J. W. Thomas, Y. Miao, C. Lee, C. Matthews, and B. Feng. “Preliminary Applications of NEAMS Codes for Multiphysics Modeling of a Heat Pipe Microreactor.” *Proceedings of the American Nuclear Society Annual 2021 Meeting* (2021).
- [3] N. E. Stauff, A. A. Abdelhameed, Y. Cao, D. Nunez, Y. Miao, K. Mo, C. Lee, C. Matthews, E. Shemon, and J. Thomas. “Applications of NEAMS Codes for Multiphysics Modeling of Several Microreactors Problems.” In *Proceedings of the American Nuclear Society Winter Conference* (2022).
- [4] A. A. Abdelhameed, Y. Cao, D. Nunez, Y. Miao, K. Mo, C. Lee, E. Shemon, and N. E. Stauff. “High-Fidelity Multiphysics Modeling of Load Following for 3-D Gas-Cooled Microreactor Assembly using NEAMS Codes.” In *Proceedings of the American Nuclear Society Winter Conference* (2022).
- [5] M.-H. Chiang, J.-Y. Wang, R.-J. Sheu, and Y.-W. H. Liu. “Evaluation of the HTTR criticality and burnup calculations with continuous-energy and multigroup cross sections.” *Nuclear Engineering and Design*, **volume 271**, pp. 327–331 (2014). URL <https://doi.org/10.1016/j.nucengdes.2013.11.056>. SI : HTR 2012.
- [6] R. Hernandez, M. Todosow, and N. R. Brown. “Micro heat pipe nuclear reactor concepts: Analysis of fuel cycle performance and environmental impacts.” *Annals of Nuclear Energy*, **volume 126**, pp. 419–426 (2019). URL <https://doi.org/10.1016/j.anucene.2018.11.050>.
- [7] P. K. Romano, C. J. Josey, A. E. Johnson, and J. Liang. “Depletion capabilities in the OpenMC Monte Carlo particle transport code.” *Annals of Nuclear Energy*, **volume 152** (2021). URL [10.1016/j.anucene.2020.107989](https://doi.org/10.1016/j.anucene.2020.107989).
- [8] J. J. Duderstadt and L. J. Hamilton. *Nuclear Reactor Analysis*, chapter 15. Wiley, New York (1976).
- [9] OECD and N. E. Agency. *Technical and Economic Aspects of Load Following with Nuclear Power Plants* (2021). URL <https://doi.org/10.1787/29e7df00-en>.
- [10] A. Isotalo and V. Sahlberg. “Comparison of Neutronics-Depletion Coupling Schemes for Burnup Calculations.” *Nuclear Science and Engineering*, **volume 179**(4), pp. 434–459 (2015). URL [10.13182/NSE14-35](https://doi.org/10.13182/NSE14-35).
- [11] K. S. Kim. “Specification for the VERA Depletion Benchmark Suite.” (2015). URL [10.2172/1256820](https://doi.org/10.2172/1256820).
- [12] “Depletion Chains.” URL <https://openmc.org/depletion-chains/>.
- [13] A. Novak, D. Andrs, P. Shriwise, J. Fang, H. Yuan, D. Shaver, E. Merzari, P. Romano, and R. Martineau. “Coupled Monte Carlo and Thermal-Fluid Modeling of High Temperature Gas Reactors Using Cardinal.” *Annals of Nuclear Energy*, **volume 177**, p. 109310 (2022). URL [10.1016/j.anucene.2022.109310](https://doi.org/10.1016/j.anucene.2022.109310).